Jurnal Ilmiah Teknik Elektro Komputer dan Informatika (JITEKI)
Vol. 8, No. 4, December 2022, pp. 520-536
ISSN: 2338-3070, DOI: 10.26555/jiteki.v8i4.24809

Terahertz Imaging Simulation Using Silicon-based Microstrip Antenna and Horn Antenna for Breast Cancer Detection

Herry Tony Andhyka, Catur Apriono, Fitri Yuli Zulkifli
Department of Electrical Engineering, Faculty of Engineering, Universitas Indonesia, Depok, 16424, Indonesia

ARTICLE INFO

Article history:

Received September 15, 2022
Revised November 2, 2022
Published December 23, 2022

Keywords:

Breast Cancer;
Horn Antenna;
Imaging;
Microstrip Antenna;
Silicon;
THz

ABSTRACT

Breast cancer is one of the most common cancers in the world that cause a lot of mortality. Early cancer detection is crucial to decrease morbidity and mortality rates worldwide. Effective treatment or early intervention is crucial before the disease becomes more incurable. This research contributes to proposing a THz imaging system for early cancer detection, especially breast cancer, by using the benefit of THz radiation. Some approaches are made differently from the previous research, such as the imaging method, the antenna type, and the material for the antenna with the expectation of producing an efficient system and better imaging results. The system consists of one microstrip antenna as a transmitter, 25 horn antenna as a receiver and a breast tissue model. All antenna is designed to meet the requirement specification. The receiver antenna will receive power from the transmitter which will vary due to the absorption of the breast model. The received power will be visualized into a 2D color image. The simulation was able to visualize an image of the breast tissue model. Received power varies from -16.280 dB to -55.241 dB which leads to different color levels to represent the model. Antenna radiation patterns also take a role to cause the phenomenon occurred that leads to differentiation of the breast tissue type. Based on the results, this research has able to simulate a THz imaging system for breast cancer. Further modification to the system can be done to improve the imaging results.

Corresponding Author:

Herry Tony Andhyka, Department of Electrical Engineering, Faculty of Engineering, Universitas Indonesia, Depok, 16424, Indonesia
Email: herry.tony11@ui.ac.id

1. INTRODUCTION

Cancer is one of the most common diseases in the world. The complexity of cancer causes a lot of mortality, with 18 million people affected and approximately 9.6 million people dead in 2018 [1], [2]. This fact makes cancer rank second as the fatal disease that leads to death. There are many types of cancer; one of the most common ones is breast cancer. Breast cancer ranks second as the most commonly occurring cancer and fifth as the most cancer mortality with 2.093 million cases and approximately 627 thousand cases that lead to death [3].

Early cancer detection is crucial to decrease morbidity and mortality rates worldwide. Effective treatment or even early intervention is crucial in this way before the disease becomes more incurable. The imaging technique is an important action in detecting the primary stage of cancer. Researchers have developed several techniques used by medics to image cancer. Computed tomography scans or CT Scans, transrectal ultrasound or TRUS, magnetic resonance imaging or MRI, positron emission tomography or PET, and single photon emission computed tomography or SPECT are some of the techniques that are commonly used nowadays [4]. Still, these techniques are not perfect because they have their drawbacks. CT scans expose high radiation to the patients, leading to DNA harm [5]. TRUS has a limitation on its low resolution and inferior contrast [6]. MRI often can not distinguish between benign disease and malignant tumors, which is fatal because of potential

false reporting [7]. PET also exposes high radiation like CT scans; even more, it has low spatial resolution and outrageous noise [8]. SPECT has a low spatial resolution but a high detection sensitivity [9].

Some research has been done prior to breast cancer imaging and classification using various methods such as deep learning, convolutional neural network, radiomics, transfer learning, fusion methods, and artificial intelligence [10]–[19] [20]–[23]. These methods are used to classify the stage of breast cancer. These methods train data using historical cancer images and then classify the current imaging results based on them. Although these are some promising techniques, those historical cance images used are images using one of the techniques mentioned before which still lack spatial resolution or are harmful to the patient therefore another imaging technique is required that can overcome these deficiencies. A better image quality resolution can lead to better classification and non-harmful imaging techniques will be safer for the patient.

Terahertz (THz) imaging operates in the 0.1-10 THz frequency range of the electromagnetic spectrum and has proposed a solution to the drawbacks [24]. THz radiation itself has some unique characteristics. THz radiation is non-ionizing, non-contact, and not harmful to human cells [24]–[26]. THz imaging also produces better images because of its high spatial resolution. For imaging context, especially cancer imaging, THz imaging is believed to be safer than other techniques while maintaining its imaging quality [27]–[29]. Thus, this technique can be used for early cancer detection, resulting in lower morbidity and mortality rates. Some research has proposed several approaches to THz imaging for cancer detection, such as a pulsed terahertz system, probe detection, a terahertz scanning mechanism, terahertz mammography, terahertz reflect emission, and other various techniques [30]–[34]. Some research has been done on THz imaging to other types of cancer such as colon cancer, lung cancer, and even the detection of living cancer cells [35]–[38]. Regarding breast cancer itself, unique characteristics of THz radiation have enabled researchers to create various techniques to image and detect breast cancer using various techniques mention befored or novel techniques [33], [34], [39]–[48]. Clearly, there are many approaches already regarding cancer imaging and detection prior to THz radiation which indicate the field of THz imaging can be explored even more to create a novel technique for better and more effective imaging.

THz imaging uses a wireless electromagnetic system. This system will consist of components, with the antenna being one of the main actors. Some researchers have considered microstrip antenna to image breast cancer using FR-4 and Rogers RT5880 as their substrate material [49]–[52]. The material used in this research is proven to be good as a substrate material in the megahertz and gigahertz spectrum, which is expected for the THz region applications. The solution to this problem is the consideration of using gallium arsenide and high-resistivity silicon as substrate material, as has been done in some studies [53]–[57]. Although it has been studied for the THz region, these materials have several drawbacks, such as narrow bandwidth and poor radiation pattern that can lead to low efficiency. Even so, these drawbacks can be minimized and overcome by using techniques such as surface micromachining and bulk machining so that these materials, such as silicon, can be used as substrate material for antennas in imaging applications.

Several studies have examined and characterized the dielectric properties of the breast tissue affected by cancer [58]–[60]. Low microwave frequencies up to 50 GHz are used in these studies. It shows that the dielectric properties in this frequency range are quite high. Later on, the dielectric properties will be used to calculate the required gain, resulting in a high gain requirement for the antenna. Even so, the dielectric properties tend to drop as the frequency increases. Thus, this makes the idea of using THz frequency for the antenna possible since it likely will require lower gain.

This study considers the translation method in the previous study to perform cancer imaging [49]. A different approach will use several antennas. Later, each antenna will provide imaging results in every part of the breast tissue without performing antenna translation. Some of these receiver antennas are horn antennas designed with a 5×5 array configuration to receive electromagnetic waves from the transmitter. The reason for using the horn antenna is its high gain. It is useful for anticipating the system's need where another type of microstrip antenna's gain offers a low gain. In addition, the horn antenna also has a directional radiation pattern and almost the same beamwidth pattern in phi = 0 degrees and phi = 90 degrees. Hence, it is good for a receiver even at small dimensions because this imaging requires directional antenna radiation patterns. This 5×5 receiver array configuration will change the translational imaging mode in the previous study because the transmitter antenna only needs to emit electromagnetic waves once received by all receiver antennas. This 5×5 receiver array configuration also indicates the scanning rate of this THz imaging simulation.

The research contribution is to propose imaging breast cancer using the benefits of THz radiation for early cancer detection to minimize cancer risk. This research also contributes by using different imaging method and antenna material that is suitable for THz radiation. This research proposes a design of a microstrip antenna using silicon as a substrate material to replace the substrate material. It operates at a frequency of 0.312 THz. where this microstrip antenna acts as a transmitter in this THz imaging system. This study also designed a horn

antenna with a 5×5 array configuration that acts as a receiver in this THz imaging system. The microstrip antenna, as a transmitter, will send electromagnetic waves that will pass through the breast tissue sample model, which the horn antenna will then receive as a receiver. This system will consist of one transmitter antenna and several receiver antennas to identify and analyze the occurring phenomena. The imaging simulation results in the received power value are visualizations of color 2D images. By analyzing the visualized image, it can be discovered whether a person has breast cancer or not. If a slight tumor is present, fast and effective treatment can be done to prevent the condition become worse.

2. METHODS

Fig. 1 shows the flowchart regarding the steps of this research. First, the specification of the system needs to be determined. The specifications are the type of antenna used, the design of the breast phantom model, the antenna specification, and other necessary details. Second, the transmitter antenna is designed by considering the type and specification needed. Third, the receiver antenna is designed also by considering the type specification needed. Some modifications will be needed during designing both antenna. Next, the imaging system is designed using the antennas that are designed in the previous steps and the breast phantom model considered before. Then, simulation is performed to obtain the received power value which then will be visualized into color 2D images. Finally, the data and imaging results will be analyzed to discover the phenomenon that occurred by this imaging simulation.

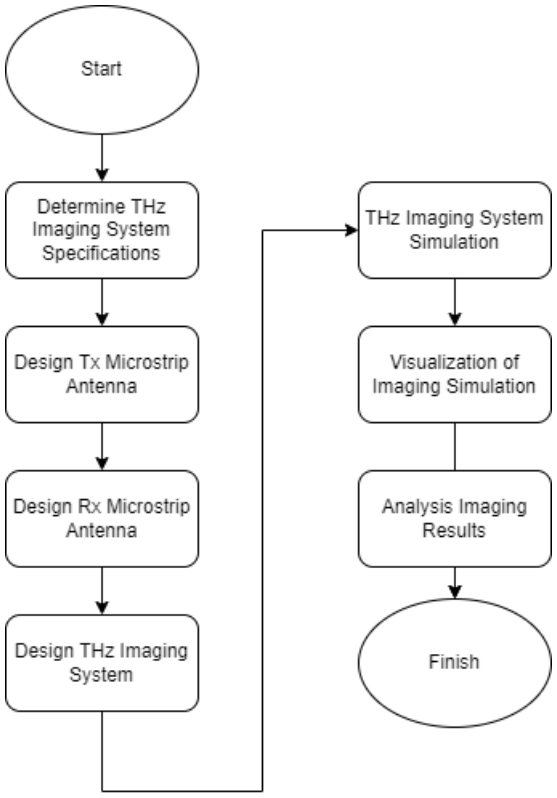

Fig. 1. Research Flowchart

There are some considerations in choosing the location of the THz spectrum range to conduct imaging. One research has considered a frequency of 312 GHz to conduct thin breast tissue imaging [61]. Other groups in France and Germany also successfully performed breast cancer imaging in the frequency range of 300–500 GHz [62]. Two groups have been researching THz imaging where the considered frequencies overlap at more than 300 GHz.

This research considers a breast tissue model based on fat, fibrous, and tumor composition. The breast cancer tumor size, measured in real life, ranges from less than 1 cm to more than 5 cm [63]. The breast tissue model considered in this work is approximately 3 mm, which is an assumed number. The tumor lies deep inside the model, which is then covered by the other two layers. Fig. 2 shows the illustration of the assumed breast tissue model. The size and the proportion of each layer of the breast tissue model is an assumption because the

exact size and proportion of breast tissue cannot be defined. When a person has breast cancer, the tumor will consume water and sodium that surround it inside the breast tissue [64]. The tumor's content will then increase its dielectric properties [65]. Because of these reasons, the genuine measure and proportion of the breast tissue and its layer can not be perfectly defined.

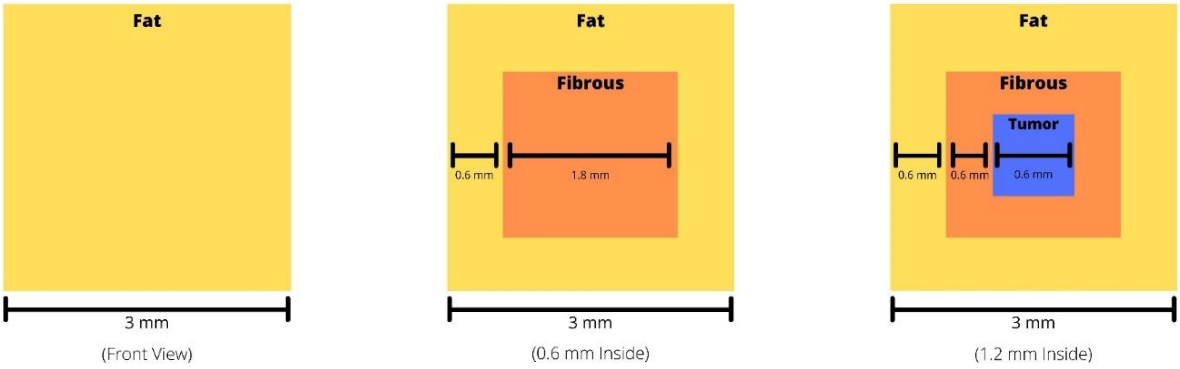

Fig. 2. (a) Outside View of the Breast Tissue Model, (b) 0.6 mm Inside the Breast Tissue Model, (c) 1.2 mm Inside the Breast Tissue Model

The antenna gain requirement for the design can be calculated using path loss calculation. Some considered losses for this condition are tissue and tumor path loss absorption [66], thermal noise on account of body temperature [66], air temperature noise [67], and a value of noise figure assumption [67]. Equation (1) is used to determine the absorption path losses [66], where α is the coefficient for absorption, d is the thickness for the assumed tissue, and e is the Euler's or natural number. Table 1 shows the summary of the total absorption path loss.

$$PL_{abs} = 10\alpha d \; log \; log \; e \tag{1}$$

Table 1. Absorption Path Loss Calculation

Type	Absorption Coefficient [cm^{-1}]	Thickness [cm]	Absorption Path Loss [dB]
Fat	27.75	0.12	14.46
Fibrous	67.91	0.12	35.39
Tumor	128.27	0.6	33.42
Total		0.3	83.27

Besides the absorption path losses, thermal noise also needs to be considered. Thermal noises consist of two types: thermal noise of body temperature and air temperature. Equation (2) is used to determine the thermal noise due to body temperature by accounting for the absorption of breast tissue [66], where $Tmol$ is the equivalent noise temperature due to tissue absorption. The parameters considered in this calculation are 310 K for reference temperature, 1 cm for thickness, and 312 GHz for frequency. After determining the condition, the calculation can be performed, resulting in 0 K for the thermal noise due to body temperature. This result implies that the body tissue does not cause any path loss. Equation (3) determines the thermal noise due to air temperature [67], where k is the Boltzmann constant, T is room temperature, and B is the antenna bandwidth. The parameters considered in this calculation are 293 K for room temperature and 5 GHz for bandwidth. After the condition is determined, the calculation results in -106.94 dB for the air temperature thermal noise. Table 2 shows the summary of the total thermal noise calculation.

$$T_{mol} = T_0\left(1 - e^{\frac{4\pi f dk}{c}}\right) \tag{2}$$

$$P_N = 10kTB \tag{3}$$

Table 2. Total Thermal Noise Calculation

Type	Temperature [K]	Noise [dB]
Human Body	0	0
Air	293	-106.94
Total		-106.94

Equation (4) is used to determine the sensitivity of the receiver antenna, where NF represents the noise figure parameter. The parameters considered in this calculation are 364.01 dB for total absorption loss, -106.94 dB for thermal noise, and 1 dB for noise figure, which is an assumed number. Considering these parameters resulted in 258.861 dB sensitivity for the receiver antenna. Table 3 summarizes the total path loss calculation showing that the loss factor can significantly reduce the radiation power. Therefore, it is required to use an antenna with high gain to create high gain radiation.

$$P_r = PL_{abs} + NF + P_N \tag{4}$$

Table 3. Total Path Losses

Types	Loss [dB]
Absorption Path Loss	83.27
Thermal Noise	-106.94
Noise Figure	1
Total	-22.66

Equation (5) is used to determine the gain specification for the antenna [67], where r is the distance of antennas, λ is the wavelength of the frequency, Pt is the transmitter antenna's power, Gt is the transmitter antenna's gain, and Gr is the receiver antenna's gain. The parameters considered in this calculation are 6 mm for antenna distance, 962 μm for wavelength, -22.66 dB for the sensitivity of the receiver antenna, and 500 mW power for the transmitter antenna. Then, The calculation can be performed by this condition, resulting in an 8.15 dB required gain.

$$r = \frac{\lambda}{4\pi}\sqrt{\frac{P_t G_t G_r}{P_r}} \tag{5}$$

The antenna also must satisfy other requirements apart from the required gain. The radiation pattern must be directed to zero degrees as close as possible for both horizontal and vertical beamwidth. A 5-degree compensation is considered for the main lobe direction. There is no standard for imaging bandwidth, so this work assumes a 5 GHz bandwidth. CST Microwave Studio Software is used to design, simulate and optimize the antenna design.

2.1. Antenna Microstrip For Transmitter

This sub-section discusses a microstrip antenna design process for the transmitter part of the system. This design considers the use of high-resistivity silicon with $\varepsilon r = 11.9$. The element used as the antenna patch is pure copper, which is good for conductor material. Fig. 3 shows the microstrip antenna design. Table 4 shows the list of antenna dimensions after the parameterization process. The design shown in Fig. 3 is the final design after some optimization and modification, such as adding inset-fed and array antennas. The modification is needed to achieve the required gain and direct beamwidth, especially the main lobe, to zero degrees to accomplish better antenna performance.

Fig. 4 shows the simulation results of the antenna design, which is the return loss. The figure shows that the antenna achieved a center frequency of 0.312 THz with -40.282 dB return loss. The bandwidth achieved based on the results is approximately 7.09 GHz, ranging from 0.308 to 0.315 GHz. This condition indicates that the antenna can operate at the desired frequency, achieve the needed bandwidth, and meet the required antenna specification.

Fig. 5 – Fig. 7 show the results from the simulated antenna design. These figures represent the radiation pattern for horizontal planes, vertical planes and far-field patterns. The antenna has an 83.9 degrees beamwidth for the horizontal beamwidth plane and 29.5 degrees beamwidth for the vertical plane. Both main-lobe beamwidth planes are also directed at 0 degrees. This result indicates the beamwidth for both planes has achieved the required antenna specification. The far-field result shows that the antenna achieves a 7.09 dB gain. The results show that all specifications required overall have almost been met. The current modification,

which is the addition of the inset-fed and array technique, is proven to achieve good antenna performance. However, the antenna performance can still improve with further modification and optimization to achieve better results in the later imaging process.

Table 4. Microstrip Transmitter Antenna Dimensions

Parameters		Label	Size (µm)
Patch	Length	Lp	165
	Width	Wp	253
	Thickness	Hp	2
Substrate	Length	Ls	1670
	Width	Ws	500
	Thickness	Hs	100
Feedline	Width	Wf	38
	Length	Lf	161
Feedline 2	Width	Wf2	51
	Length	Lf2	437
Feedline 3	Width	Wf3	57
	Length	Lf3	471
Inset Fed	Width	Gpf	2
	Length	Fi	63

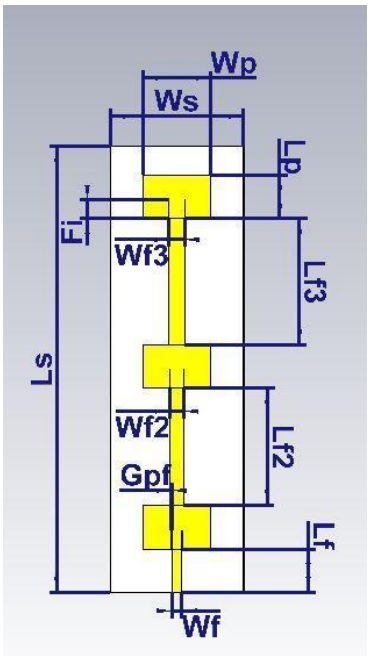

Fig. 3. Top View of the Microstrip Antenna Design

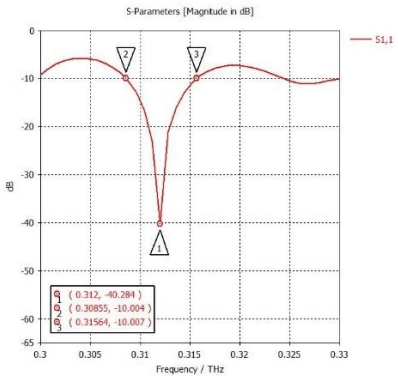

Fig. 4. Return Loss Result of the Microstrip Antenna

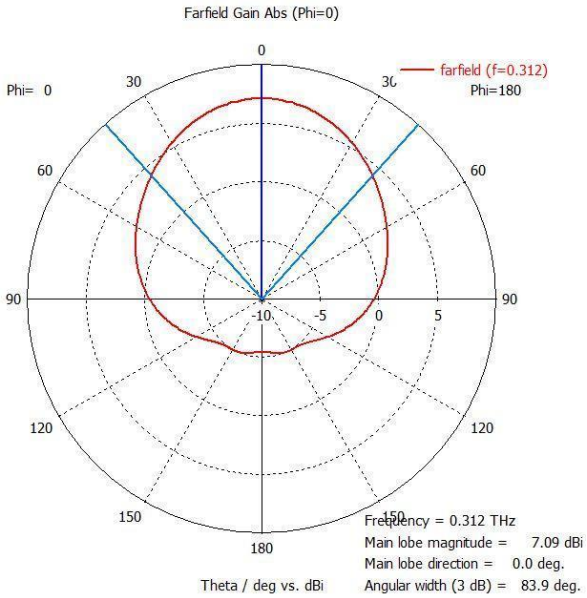

Fig. 5. The Horizontal Plane Pattern of the Microstrip Antenna

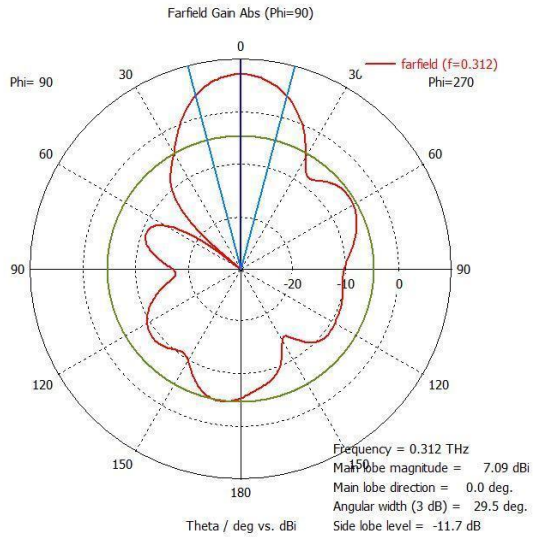

Fig. 6. The Vertical Pattern of the Microstrip Antenna

The antenna design has met the overall specification required to work properly. The antenna beamwidth can be furthermore considered to achieve better imaging results [68]. A focused power propagation can be achieved by utilizing a small beamwidth from the antenna to achieve optimal propagation through the tissue model. Another issue that can be seen from the results is that the horizontal beamwidth is larger than the vertical beamwidth. The solution to this problem is adding more elements horizontally to minimize the horizontal beamwidth to improve the antenna performance. Based on the radiation pattern results, it is clear that the antenna has not reached its optimum gain because its total efficiency is below 0 dB, which means some power is trapped inside the substrate. A 0 dB efficiency is considered so the antenna can reach its potential gain and optimum propagation.

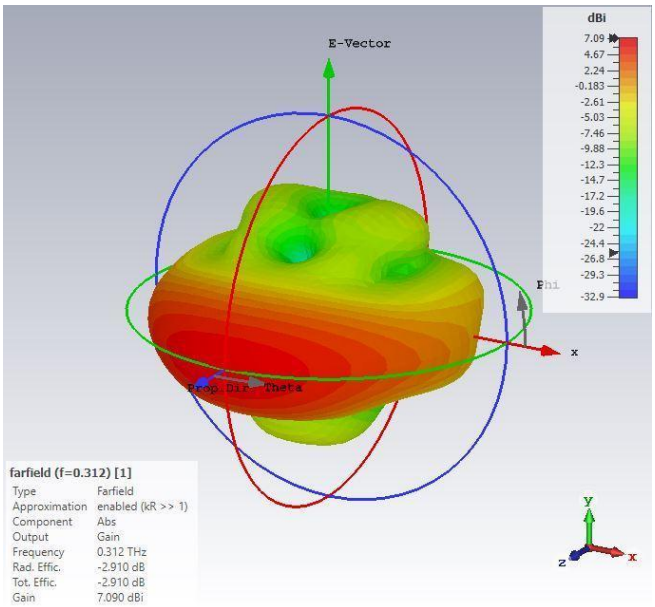

Fig. 7. Far-Field Result of the Microstrip Antenna

2.2. Antenna Horn For Receiver

The antenna that is designed as a receiver antenna is a horn antenna. This antenna is designed using the horn antenna demo feature in the CST Microwave Studio software, which can automatically construct a horn antenna with several parameters that the author can change. The horn antenna configuration can be seen in Fig 8. The dimensions of the horn antenna can be seen in Table 5. The dimensions listed in Table 5 are the dimensions after the iteration and optimization process.

Table 5. Horn Receiver Antenna Dimensions

Parameters	Label	Size (µm)
Waveguide Width	Ww	577
Waveguide Height	Wh	577
Horn Length	Hl	15.9
Wall Thickness	Wt	2

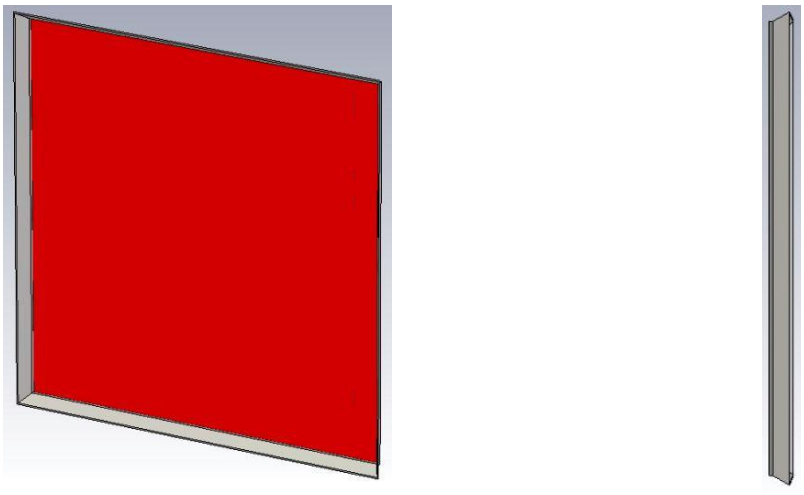

(a) (b)

Fig. 8. (a) Top View of the Horn Antenna Design, (b) Side View of the Horn Antenna

Fig. 9 shows the simulation results of the antenna design, which is the return loss. The figure shows that the antenna achieved a center frequency of 0.312 THz with -18.187 dB return loss. This condition indicates that the antenna can operate at the desired frequency and meet the required antenna specification.

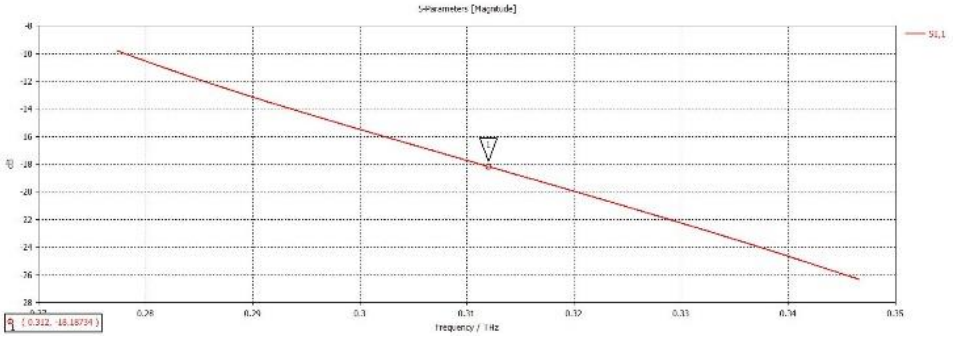

Fig. 9. Return Loss Result of the Horn Antenna

Fig. 10 – Fig.11 show the results from the antenna design that has been simulated. These figures represent the radiation pattern for both horizontal and vertical planes. The antenna has a 74.9 degrees beamwidth for the horizontal plane and 78.4 degrees for the vertical plane. This result indicates the beamwidth for both planes has achieved the required antenna specification.

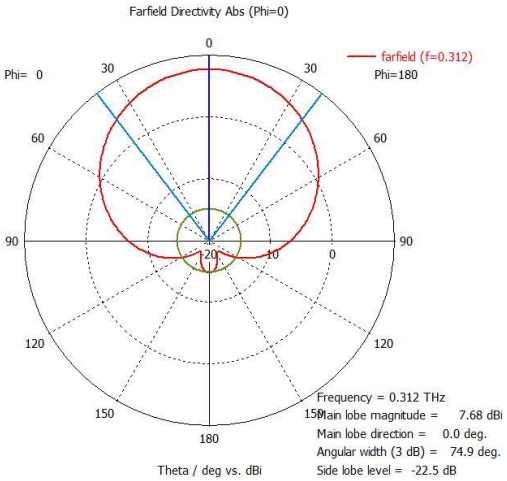

Fig. 10. The Horizontal Plane Pattern of the Horn Antenna

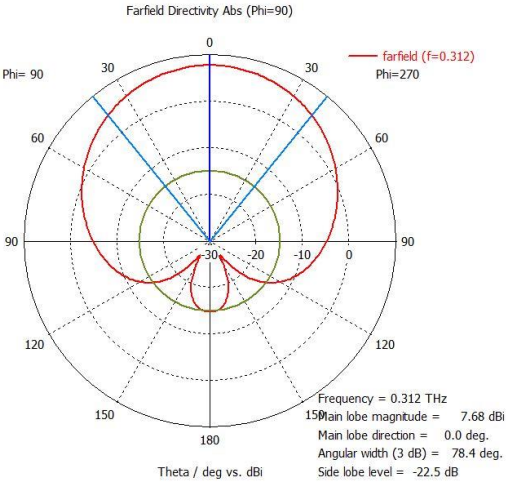

Fig. 11. The Vertical Pattern of the Horn Antenna

Fig. 12 shows the far-field simulation results of the proposed antenna. The results show that the antenna achieves a 7.68 dB gain. Overall, the horn antenna configuration met all the specifications. Later, this horn

antenna will also be arrayed with 5×5 components on the receiver side. Later, the total gain of the antenna will increase so that electromagnetic waves from the transmitter side can be received on the receiver side.

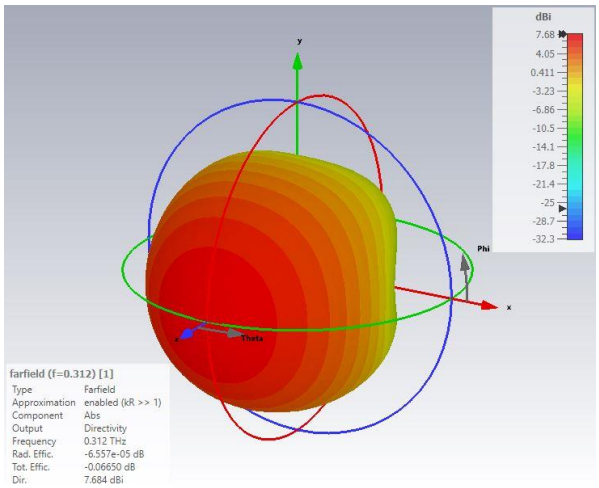

Fig. 12. Far-Field Result of the Horn Antenna

3. RESULTS AND DISCUSSION

THz imaging simulation design is needed to determine how the system schematic is created and executed. The scheme used in this study uses 1 transmitter antenna in the form of a microstrip antenna and 25 receiver antennas in the form of a horn antenna. The transmitter and receiver antennas are placed at a distance of 1.5 mm from the phantom. The total distance between the transmitter and receiver is 6 mm.

The transmitter antenna has a reactive near field at a distance of less than 1 mm, a radiating near field or fresnel region at a distance of 1mm to 5.8 mm, and a far field at a distance greater than 5.8 mm. As for the receiver antenna, each antenna has a reactive near field at a distance of less than 0.29 mm, a radiating near field or fresnel region at a distance of 0.29 mm to 0.74 mm, and a far-field at a distance greater than 0.74 mm. So it can be said that this THz imaging simulation is in the far-field region of the two antennas. This simulation will produce data from return loss values which will later be visualized into 2D color images. A schematic of THz imaging in 3D can be seen in Fig. 13.

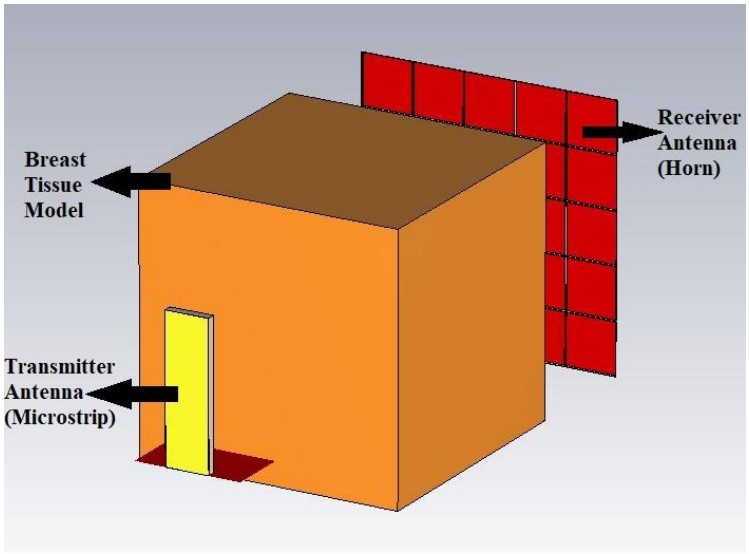

Fig. 13 THz Imaging Scheme with Phantom

The simulation results in this imaging are 25 power values received by each receiver antenna. Each received power value will represent 25 points in the imaged phantom model. All the data will then be visualized as a kind of heat map that is simulated and visualized. The power values received from the three components can be seen in Table 6.

Table 6. Received Power of Each Receiver Antenna

Y\X (mm)	0.6	1.2	1.8	2.4	3
0.6	-26.513	-32.489	-55.241	-35.169	-28.733
1.2	-25.078	-20.038	-19.571	-19.572	-24.706
1.8	-24.008	-16.280	-17.345	-18.434	-22.619
2.4	-25.334	-22.876	-20.536	-22.862	-25.605
3.0	-34.392	-25.462	-50.9	-35.974	-30.478

Fig. 14 shows a two-dimensional image of Terahertz imaging which is constructed from 25 power values received by 25 receivers. In contrast, Fig 15 shows a two-dimensional image of the phantom model that is used as a reference. Visually, the imaging results in this simulation have not succeeded in representing the phantom model well. This condition can be seen from the failure of the imaging results to distinguish the three layers properly. It can be seen that the red areas are quite overlapping in the middle, whereas there should be only 1 point in the middle which is solid red, to represent the tumor. Likewise, the fibrous and fat parts surrounding it have not been successfully represented properly, as seen from the spread of orange on the outside, which should be yellow to represent fat tissue.

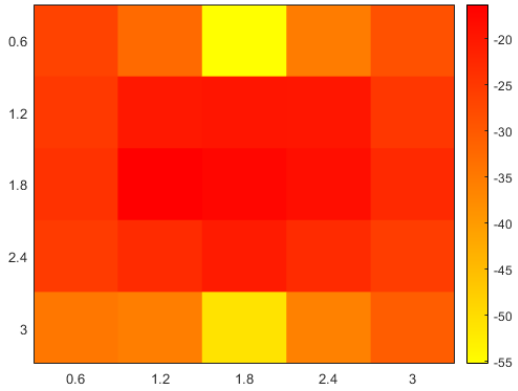

Fig. 14. Imaging Results of the THz Imaging Simulation

Fig. 15. Reference Results of the Phantom Model

One of the causes of this poor imaging result is the result of the values at (1.8, 0.6) and at (1.8, 3) which are -55.241 dB and -50.9 dB, are quite far from the surrounding points, especially for points that represent fat tissue. The received power value, which is quite far away, creates a gap in the dB level represented by the color. The received power value, which is quite small at these two points, can be analyzed from the far field of these two points, which can be seen in Fig. 16 – Fig. 19.

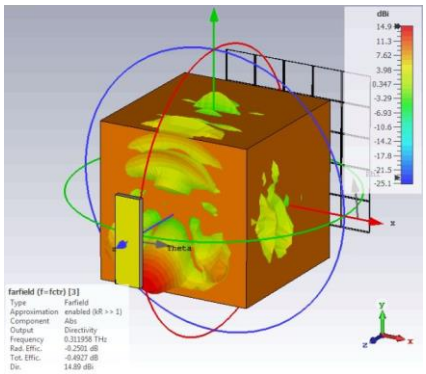

Fig. 16. Far-Field Results at Port Number 3

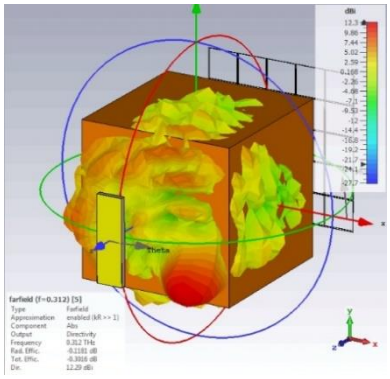

Fig. 17. Far-Field at Port Number 23

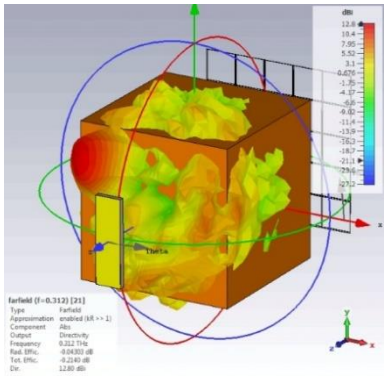

Fig. 18. Far-Field at Port Number 5

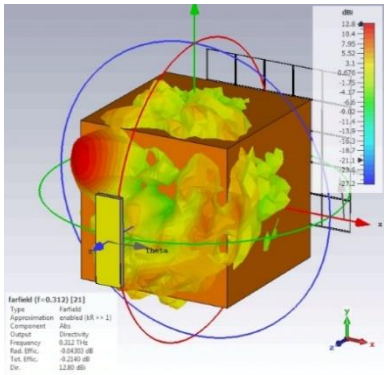

Fig. 19. Far-Field at Port Number 21

Fig. 16 – Fig. 17 represents the far-field on ports 3 and 23 at points (1.8, 0.6) and (1.8, 3), which have a fairly small value of received power. It can be seen in the image that the main lobe does not completely pass through the center of the phantom, which indicates that the tumor tissue does not completely absorb the wave, so the power value received is still quite small. Fig. 18 – Fig. 19 represents the far-field on ports 5 and 21, namely at points (0.6 , 0.6) and at (3, 3). Farfield on ports 5 and 21 was chosen in this analysis because it has a received power value much greater than the power value obtained on ports 3 and 23. It can be seen in the figure that most of the whole main lobe in the image passes through the middle compared to the main lobe on ports 3 & 23, which indicates that the tumor tissue almost completely absorbs the wave inside so that the received power value is greater than the ports 3 and 23. One of the other causes that cause this imaging result is not good is seen from the power value, which is quite the same in the middle. This condition is caused by the farfield of the transmitter antenna, which can be seen in Fig. 6. In the figure, the farfield pattern tends to be in the horizontal part. This condition causes the received power value to be large and centered in the middle. In addition, the picture shows the upper farfield pattern is quite different from the lower one. This condition causes a difference in the received power value between points $y = 0.6$ and 1.2 and $y = 2.4$ and 3.

Compared to the related previous studies which consider antenna in the imaging system [49]–[52] a different approach is considered in this research. In the previous study, the system consist also with the same main component but with a different imaging method. Translation method is used, which is both transmitter and receiver antenna propagate wave and translate several distances horizontally and vertically to obtain receiver power value to visualize image. In this research, both transmitter and receiver antenna do not need to translate, instead transmitter antenna propagate wave that is received by the receiver antenna with additional number of receiver antenna for its spatial resolution. Between these two approaches, the previous study is more complicated to be implicated in real-life situation because the antenna size is very small and it will be hard to move the antenna freely. While this research proposes a simpler way for imaging which is more possible to be implemented in real life. As for the imaging results, both techniques are able to differentiate breast tissue types based on the received power value but still need more modification to improve their imaging results.

Compared to actual common techniques that are used nowadays as mentioned before such as MRI, CT Scan, and others, some of the techniques will provide better imaging results than the current results of this results [69]. But in other optics, it is known that imaging using THz radiation will be safe than other current techniques. For the complexity of the techniques, the common techniques used nowadays are using expensive complicated, and massive components or equipment while the proposed techniques in this research are believed to be simpler and use smaller components which is possible to be implemented and will be easier to use. Despite that, the proposed technique needs to improve its imaging results in order to be used in real life.

The main objective of this research is to image breast cancer model using the proposed system. The results indicate that this research can differentiate breast tissue type according to varying received power value data obtained based on the simulation. In spite of that, the imaging process has not been able to produce perfect imaging results that are hoped for. According to the findings, the propagated wave may cause the imperfection of the imaging results. Despite the other things that have not been found which can cause the imaging results, this proposed technique is a promising solution that can address the deficiencies of currently available techniques but further research needs to be done to improve its whole imaging system.

4. CONCLUSION

This research has proposed a terahertz imaging system for breast cancer imaging. The system consists of one microstrip antenna as a transmitter, 25 horn antenna as a receiver and a breast tissue model. All antennas have been designed and simulated to meet the required specification. The THz imaging system has been able to image the breast tissue model. The image was created by visualizing the received power value from each receiver antenna. Received power varies from -16.280 dB to -55.241 dB, leading to different color levels representing the model. Analysis based on the results has been done to observe the phenomenon. This research can be used as a reference for further development to improve the result of this promising imaging technique. Improvement can be done by modifying the antenna both the transmitter and receiver so both antenna has better performance including their gain and radiation pattern which can lead to better image results. Imaging scheme details such as breast phantom model design and distance between each component of the system can be considered more because the actual size of the breast phantom is different for everyone and antenna placement can be possible done in actual conditions.

Acknowledgments

Universitas Indonesia supports this research through International Indexed Publication (PUTI) Q1 Grant, the year 2022, number: NKB-500/UN2.RST/HKP.05.00/2022.

REFERENCES

[1] "Cancer." [Online]. Available: https://www.who.int/news-room/fact-sheets/detail/cancer. [Accessed: 04-Apr-2020].
[2] "All Cancers." [Online]. Available:. [Accessed: 04-Apr-2020].
[3] "Breast." [Online]. Available:https://gco.iarc.fr/today/data/factsheets/cancers/20-Breast-fact-sheet.pdf. [Accessed: 04-Apr-2020].
[4] J. V. Frangioni, "New technologies for human cancer imaging," *J. Clin. Oncol.*, vol. 26, no. 24, pp. 4012–4021, 2008, https://doi.org/10.1200/JCO.2007.14.3065.
[5] K. E. Darras, *et al.*, "Integrated virtual and cadaveric dissection laboratories enhance first year medical students' anatomy experience: a pilot study," *BMC medical education*, vol. 19, no. 1, pp. 1-6. 2019, https://link.springer.com/article/10.1186/s12909-019-1806-5.
[6] "MRI | CancerQuest." [Online]. Available: https://www.cancerquest.org/patients/detection-and-diagnosis/magnetic-resonance-imaging-mri. [Accessed: 04-Apr-2020].
[7] J. J. Vaquero and P. Kinahan, "Positron Emission Tomography: Current Challenges and Opportunities for Technological Advances in Clinical and Preclinical Imaging Systems," *Annu. Rev. Biomed. Eng.*, vol. 17, no. 1, pp. 385–414, Dec. 2015, https://doi.org/10.1146/annurev-bioeng-071114-040723.
[8] G. L. Gravina *et al.*, "Advances in imaging and in non-surgical salvage treatments after radiorecurrence in prostate cancer: What does the oncologist, radiotherapist and radiologist need to know?," *Eur. Radiol*, vol. 22, no. 12, pp. 2848–2858, 2012, https://doi.org/10.1007/s00330-012-2546-7.
[9] M. . Khalil, J. . Tremoleda, T. . Bayomy, and W. Gsell, "Molecular SPECT Imaging: An Overview," *Int. J. Mol. Imaging*, vol. 2011, pp. 1–15, 2011, https://doi.org/10.1155/2011/796025.
[10] M. Li, "Research on the detection method of breast cancer deep convolutional neural network based on computer aid," *Proc. IEEE Asia-Pacific Conf. Image Process. Electron. Comput. IPEC 2021*, pp. 536–540, Apr. 2021, https://doi.org/10.1109/IPEC51340.2021.9421338.
[11] N. Wu *et al.*, "Deep Neural Networks Improve Radiologists' Performance in Breast Cancer Screening," *IEEE Trans. Med. Imaging*, vol. 39, no. 4, pp. 1184–1194, Apr. 2020, https://doi.org/10.1109/TMI.2019.2945514.
[12] G. Chen, Y. Chen, Z. Yuan, X. Lu, X. Zhu, and W. Li, "Breast Cancer Image Classification based on CNN and Bit-Plane slicing," *2019 Int. Conf. Med. Imaging Phys. Eng. ICMIPE 2019*, Nov. 2019, https://doi.org/10.1109/ICMIPE47306.2019.9098216.
[13] Y. Amkrane, M. El Adoui, and M. Benjelloun, "Towards Breast Cancer Response Prediction using Artificial Intelligence and Radiomics," *Proc. 2020 5th Int. Conf. Cloud Comput. Artif. Intell. Technol. Appl. CloudTech 2020*, Nov. 2020, https://doi.org/10.1109/CloudTech49835.2020.9365890.
[14] M. Ahmed and M. R. Islam, "A Multiple-Input Based Convolutional Neural Network in Breast Cancer Classification from Histopathological Images," *24th Int. Conf. Comput. Inf. Technol. ICCIT 2021*, 2021, https://doi.org/10.1109/ICCIT54785.2021.9689856.
[15] S. Misra *et al.*, "Bi-Modal Transfer Learning for Classifying Breast Cancers via Combined B-Mode and Ultrasound Strain Imaging," *IEEE Trans. Ultrason. Ferroelectr. Freq. Control*, vol. 69, no. 1, pp. 222–232, Jan. 2022, https://doi.org/10.1109/TUFFC.2021.3119251.
[16] B. Gong *et al.*, "BI-Modal Ultrasound Breast Cancer Diagnosis Via Multi-View Deep Neural Network SVM," *Proc. -Int. Symp. Biomed. Imaging*, vol. 2020-April, pp. 1106–1110, Apr. 2020, https://doi.org/10.1109/ISBI45749.2020.9098438.
[17] E. Hamdy, M. S. Zaghloul, and O. Badawy, "Deep learning supported breast cancer classification with multi-modal image fusion," *2021 22nd Int. Arab Conf. Inf. Technol. ACIT 2021*, 2021, https://doi.org/10.1109/ACIT53391.2021.9677099.
[18] Z. Yuan, G. Chen, Q. Chen, W. Li, and S. Long, "Breast Cancer Image Classification Based on CNN Classifier," *Proc. - IEEE Congr. Cybermatics 2020 IEEE Int. Conf. Internet Things, iThings 2020, IEEE Green Comput. Commun. GreenCom 2020, IEEE Cyber, Phys. Soc. Comput. CPSCom 2020 IEEE Smart Data, SmartD*, pp. 921–925, 2020, https://doi.org/10.1109/iThings-GreenCom-CPSCom-SmartData-Cybermatics50389.2020.00143.
[19] Z. Jadah, Alfitouri, M. Aisha Chantar, Hamouda Amarif, and A. A. Aeshah, "Breast Cancer Classification Using Deep Convolutional Neural Networks," in *International Conference on Engineering & MIS (ICEMIS)*, pp. 1–6. 2022, https://doi.org/10.1109/ICEMIS56295.2022.9914251.
[20] M. Yamakawa, T. Shiina, K. Tsugawa, N. Nishida, and M. Kudo, "Deep-learning framework based on a large ultrasound image database to realize computer-aided diagnosis for liver and breast tumors," *2021 IEEE Int. Ultrason. Symp.*, pp. 1–4, Sep. 2021, https://doi.org/10.1109/IUS52206.2021.9593518.
[21] G. Jayandhi, J. S. Leena Jasmine, R. Seetharaman, and S. Mary Joans, "Breast Cancer Prediction Based on Mammographic data by Hybrid Resnet and Decision Tree," *Int. Conf. Sustain. Comput. Data Commun. Syst. ICSCDS 2022 - Proc.*, pp. 234–238, 2022, https://doi.org/10.1109/ICSCDS53736.2022.9760754.
[22] Y. Zhou *et al.*, "A radiomics approach with CNN for shear-wave elastography breast tumor classification," *IEEE Trans. Biomed. Eng.*, vol. 65, no. 9, pp. 1935–1942, 2018, https://doi.org/10.1109/TBME.2018.2844188.
[23] S. S. Boudouh and M. Bouakkaz, "Breast Cancer: Using Deep Transfer Learning Techniques AlexNet Convolutional Neural Network For Breast Tumor Detection in Mammography Images," *2022 7th Int. Conf. Image Signal Process. their Appl. ISPA 2022 - Proc.*, 2022, https://doi.org/10.1109/ISPA54004.2022.9786351.
[24] Y. Zhang, *et al.*, "Continuous-wave THz imaging for biomedical samples," *Applied Sciences*, vol. 11, no. 1, p. 71, 2020, https://www.mdpi.com/2076-3417/11/1/71.

[25] J. B. Baxter and G. W. Guglietta, "Terahertz Spectroscopy," *Anal. Chem.*, vol. 83, no. 12, pp. 4342–4368, Jun. 2011. https://doi.org/10.1021/ac200907z.
[26] M. Wan, J. J. Healy, and J. T. Sheridan, "Terahertz phase imaging and biomedical applications," *Opt. Laser Technol.*, vol. 122, p. 105859, Feb. 2020, https://doi.org/10.1016/j.optlastec.2019.105859.
[27] M. Gezimati and G. Singh, "Advances in Terahertz Instrumentation and Technology for Cancer Applications," pp. 1–2, Sep. 2022, https://doi.org/10.1109/IRMMW-THz50927.2022.9896072.
[28] T. Skotnicki and W. Knap, "Terahertz technologies and applications," *Proc. 26th Int. Conf. "Mixed Des. Integr. Circuits Syst. Mix. 2019*, pp. 34–37, Jun. 2019, https://doi.org/10.23919/MIXDES.2019.8787160.
[29] Y. He, Y. Chen, L. Zhang, S. W. Wong, and Z. N. Chen, "An overview of terahertz antennas," *China Commun.*, vol. 17, no. 7, pp. 124–165, Jul. 2020, https://doi.org/10.23919/J.CC.2020.07.011.
[30] K. Liu, Q. Sun, X. Chen, A. I. Hernandez-Serrano, and E. Pickwell-Macpherson, "Highly sensitive terahertz imaging method for paraffin embedded cancer samples," *Int. Conf. Infrared, Millimeter, Terahertz Waves, IRMMW-THz*, vol. 2019-Septe, 2019, https://doi.org/10.1109/IRMMW-THz.2019.8874532.
[31] H. Chen *et al.*, "High-sensitivity in vivo THz fiber-scanning mammography of early breast cancer in nude mice," *Opt. InfoBase Conf. Pap.*, pp. 5–6, 2011, https://doi.org/10.1364/CLEO_SI.2011.CThV5.
[32] A. Portieri, M. Grootendorst, and T. Fitzgerald, "Intra-operative terahertz probe for detection of breast cancer," *2015 8th UK, Eur. China Millim. Waves THz Technol. Work. UCMMT 2015*, pp. 4–5, 2016, https://doi.org/10.1109/UCMMT.2015.7460611.
[33] A. Shariffar, T. Bowman, C. Lai, M. Huang, M. El-Shenawee, and K. Bailey, "Modelling the Interaction of THz Waves with Breast Cancer Tissues," *2018 IEEE Antennas Propag. Soc. Int. Symp. Usn. Natl. Radio Sci. Meet. APSURSI 2018 - Proc.*, no. 1, pp. 1843–1844, 2018, https://doi.org/10.1109/APUSNCURSINRSM.2018.8609091.
[34] T. Bowman, M. El-Shenawee, and K. Bailey, "Terahertz Imaging of Transgenic Murine Breast Cancer Tumors," *2018 IEEE Antennas Propag. Soc. Int. Symp. Usn. Natl. Radio Sci. Meet. APSURSI 2018 - Proc.*, pp. 901–902, 2018, https://doi.org/10.1109/APUSNCURSINRSM.2018.8609230.
[35] Y. Cao, J. Chen, P. Huang, W. Ge, D. Hou, and G. Zhang, "Inspecting human colon adenocarcinoma cell lines by using terahertz time-domain reflection spectroscopy," *Spectrochim. Acta Part A Mol. Biomol. Spectrosc.*, vol. 211, pp. 356–362, Mar. 2019, https://doi.org/10.1016/j.saa.2018.12.023.
[36] S. H. Gupta, S. Goel, M. Kumar, A. Rajawat, and B. Singh, "Design of terahertz antenna to detect lung cancer and classify its stages using machine learning," *Optik (Stuttg).*, vol. 249, p. 168271, Jan. 2022, https://doi.org/10.1016/j.ijleo.2021.168271.
[37] X. Yan *et al.*, "The terahertz electromagnetically induced transparency-like metamaterials for sensitive biosensors in the detection of cancer cells," *Biosens. Bioelectron.*, vol. 126, pp. 485–492, Feb. 2019, https://doi.org/10.1016/j.bios.2018.11.014.
[38] Z. Zhang *et al.*, "Terahertz circular dichroism sensing of living cancer cells based on microstructure sensor," *Anal. Chim. Acta*, vol. 1180, p. 338871, Oct. 2021, https://doi.org/10.1016/j.aca.2021.338871.
[39] M. Boutaayamou, D. Cerica, and J. G. Verly, "Terahertz pulsed imaging of dehydrated human breast cancer samples," *Int. Conf. Infrared, Millimeter, Terahertz Waves, IRMMW-THz*, vol. 2020-November, pp. 65–66, Nov. 2020, https://doi.org/10.1109/IRMMW-THz46771.2020.9370383.
[40] T. Chavez, N. Vohra, J. Wu, M. El-Shenawee, and K. Bailey, "Spatial Image Segmentation for Breast Cancer Detection in Terahertz Imaging," *2020 IEEE Int. Symp. Antennas Propag. North Am. Radio Sci. Meet. IEEECONF 2020 - Proc.*, pp. 1157–1158, Jul. 2020, https://doi.org/10.1109/IEEECONF35879.2020.9330445.
[41] P. Kaurav, S. Koul, and A. Basu, "Design of Sub-Terahertz Waveguide Iris Probe for Breast Cancer Tumor Margin Assessment," *2021 IEEE MTT-S Int. Microw. RF Conf. IMARC 2021*, 2021, https://doi.org/10.1109/IMaRC49196.2021.9714693.
[42] N. Vohra, T. Bowman, M. El-Shenawee, and K. Bailey, "Image reconstruction of freshly excised human breast tumors using terahertz electrical properties," *2019 IEEE Int. Symp. Antennas Propag. Usn. Radio Sci. Meet. APSURSI 2019 - Proc.*, pp. 571–572, Jul. 2019, https://doi.org/10.1109/APUSNCURSINRSM.2019.8888949.
[43] T. Bowman, M. El-Shenawee, and K. Bailey, "Challenges in Terahertz Imaging of Freshly Excised Human Breast Tumors," *2018 IEEE Antennas Propag. Soc. Int. Symp. Usn. Natl. Radio Sci. Meet. APSURSI 2018 - Proc.*, pp. 13–14, 2018, https://doi.org/10.1109/APUSNCURSINRSM.2018.8608576.
[44] C. Oldfield, T. Bowman, and M. El-Shcnawcc, "Development of Tunable Breast Tissue Phantoms for Terahertz Imaging," *2018 IEEE Antennas Propag. Soc. Int. Symp. Usn. Natl. Radio Sci. Meet. APSURSI 2018 - Proc.*, pp. 1397–1398, 2018, https://doi.org/10.1109/APUSNCURSINRSM.2018.8608493.
[45] N. Vohra, M. El-Shenawee, and K. Bailey, "Dehydration Approach for Enhancing Terahertz Detection of Cancer in Freshly Excised Breast Tumors," *2020 IEEE Int. Symp. Antennas Propag. North Am. Radio Sci. Meet. IEEECONF 2020 - Proc.*, pp. 43–44, Jul. 2020, https://doi.org/10.1109/IEEECONF35879.2020.9330034.
[46] T. Bowman, M. El-Shenawee, and K. Bailey, "Terahertz Time-Domain Pulsed Spectroscopy of Human Breast Cancer Tissues," *2018 IEEE Antennas Propag. Soc. Int. Symp. Usn. Natl. Radio Sci. Meet. APSURSI 2018 - Proc.*, pp. 1067–1068, 2018, https://doi.org/10.1109/APUSNCURSINRSM.2018.8608929.
[47] N. Vohra, M. El-Shenawee, and K. Bailey, "Terahertz Imaging of ENU Injected Sprague Dawley Rat Breast Cancer Tumors," *2021 IEEE Int. Symp. Antennas Propag. North Am. Radio Sci. Meet. APS/URSI 2021 - Proc.*, pp. 585–586, 2021, https://doi.org/10.1109/APS/URSI47566.2021.9703938.

[48] N. Vohra *et al.*, "Terahertz Imaging of Breast Cancer using Human and Animal Models," *2021 IEEE Conf. Antenna Meas. Appl. CAMA 2021*, pp. 368–371, 2021, https://doi.org/10.1109/CAMA49227.2021.9703666.
[49] I. Nurfitri and C. Apriono, "Radiation Beamwidth Characterization to Enhance Terahertz Imaging Quality for Cancer Detection," in *Proceedings - CAMA 2019: IEEE International Conference on Antenna Measurements and Applications*, pp. 207–209, 2019, https://doi.org/10.1109/CAMA47423.2019.8959591.
[50] M. V. Hidayat and C. Apriono, "Design of 0.312 THz microstrip linear array antenna for breast cancer imaging application," in *International Conference on Signals and Systems, ICSigSys 2018 - Proceedings, 2018*, pp. 224–228, 2018, https://doi.org/10.1109/ICSIGSYS.2018.8372671.
[51] I. Nurfitri and C. Apriono, "Rectangular Linear Array Microstrip Antenna Design for Terahertz Imaging," in *2019 International Conference on Information and Communications Technology (ICOIACT)*, pp. 719–722, 2019, https://doi.org/10.1109/ICOIACT46704.2019.8938556.
[52] I. Nurfitri and C. Apriono, "Rectangular microstrip array antenna for enhancing terahertz imaging quality," *2nd IEEE Int. Conf. Innov. Res. Dev. ICIRD 2019*, Jun. 2019, https://doi.org/10.1109/ICIRD47319.2019.9074652.
[53] N. K. Nikolova, M. Ravan, and R. K. Amineh, "Chapter Six - Substrate-Integrated Antennas on Silicon," in *Silicon-Based Millimeter-wave Technology*, vol. 174, M. J. B. T.-A. in I. and E. P. Deen, Ed. Elsevier, pp. 391–458, 2012, https://doi.org/10.1016/B978-0-12-394298-2.00006-5.
[54] A. Mostajeran, H. Aghasi, S. M. H. Naghavi, and E. Afshari, "Fully Integrated Solutions for High Resolution Terahertz Imaging (Invited)," *Proc. Cust. Integr. Circuits Conf.*, pp. 1-8, Apr. 2019, https://doi.org/10.1109/CICC.2019.8780262.
[55] Z. Wang, "Silicon-based Integrated Circuits for Terahertz Fundamental Transceivers," *2019 Int. Conf. Microw. Millim. Wave Technol. ICMMT 2019 - Proc.*, May 2019, https://doi.org/10.1109/ICMMT45702.2019.8992566.
[56] J. Oberhammer, "Overview and recent achievements in silicon micromachining for THz systems," *Proc. Eur. Microw. Conf. Cent. Eur. EuMCE 2019*, pp. 23–26, 2019, https://doi.org/10.1016/j.isci.2022.105217.
[57] Q. Qiu *et al.*, "High sensitivity of room-temperature terahertz photodetector based on silicon," *iScience*, vol. 25, no. 10, p. 105217, Oct. 2022, https://doi.org/10.1109/IMWS-AMP.2017.8247371.
[58] S. Di Meo *et al.*, "Dielectric characterization of material for 3D-printed breast phantoms up to 50 GHz: Preliminary experimental results," *2017 IEEE MTT-S Int. Microw. Work. Ser. Adv. Mater. Process. RF THz Appl. IMWS-AMP 2017*, vol. 2018-Janua, no. September, pp. 1–3, 2018, https://doi.org/10.1111/1759-7714.12605.
[59] Y. Cheng and M. Fu, "Dielectric properties for non-invasive detection of normal, benign, and malignant breast tissues using microwave theories," *Thorac. Cancer*, vol. 9, no. 4, pp. 459–465, 2018, https://doi.org/10.1109/IMWS-AMP.2017.8247408.
[60] S. Di Meo *et al.*, "Experimental validation of the dielectric permittivity of breast cancer tissues up to 50 GHz," *2017 IEEE MTT-S Int. Microw. Work. Ser. Adv. Mater. Process. RF THz Appl. IMWS-AMP 2017*, vol. 2018-Janua, no. September, pp. 1–3, 2018, https://doi.org/10.1109/IMWS-AMP.2017.8247408.
[61] Son, J. H. (Ed.), *Terahertz biomedical science and* technology, CRC Press, 2014, https://books.google.co.id/books?id=2IWhAwAAQBAJ.
[62] A. Al-Ibadi *et al.*, "THz spectroscopy and imaging for breast cancer detection in the 300-500 GHz range," *Int. Conf. Infrared, Millimeter, Terahertz Waves, IRMMW-THz*, no. Spp 1857, p. 3853, 2017, https://doi.org/10.1109/IRMMW-THz.2017.8067037.
[63] H. G. Welch, P. C. Prorok, A. J. O'Malley, and B. S. Kramer, "Breast-cancer tumor size, overdiagnosis, and mammography screening effectiveness," *N. Engl. J. Med.*, vol. 375, no. 15, pp. 1438–1447, 2016, https://doi.org/10.1056/NEJMoa1600249.
[64] M. O'Halloran, D. Byrne, R. C. Conceição, E. Jones, and M. Glavin, "Anatomy and Dielectric Properties of the Breast and Breast Cancer," in *An Introduction to Microwave Imaging for Breast Cancer Detection. Biological and Medical Physics, Biomedical Engineering. Springer, Cham.*, 2016, https://doi.org/10.1007/978-3-319-27866-7_2.
[65] M. Hussein, F. Awwad, D. Jithin, H. El Hasasna, K. Athamneh, and R. Iratni, "Breast cancer cells exhibits specific dielectric signature in vitro using the open-ended coaxial probe technique from 200 MHz to 13.6 GHz," *Sci. Rep.*, vol. 9, no. 1, pp. 1–8, 201, https://doi.org/10.1038/s41598-019-41124-1.
[66] A. A. N. Chopra, K. Yang, Q. H. Abbasi, K. A. Qaraqe, M. Philpott, "THz Time-Domain Spectroscopy of Human Skin Tissue for In-Body Nanonetworks," *IEEE Trans. Terahertz Sci. Technol.*, vol. 6, no. 6, pp. 803–809, 2016, https://doi.org/10.1109/TTHZ.2016.2599075.
[67] E. Ibarra-Medel, M. Velázquez, D. Ferrusca, and S. Kurtz, "Design and construction of a Low-Noise L-Band Amplifier for the Tulancingo I radio Telescope," *In 2022 IEEE Latin American Electron Devices Conference (LAEDC)* , pp. 1-4, 2022, https://ieeexplore.ieee.org/abstract/document/9908176.
[68] T. Binder, "1.6.3 Image Resolution | 123sonography." [Online]. Available: https://www.123sonography.com/content/163-image-resolution. [Accessed: 26-Aug-2020].
[69] Z. S. Lima, M. R. Ebadi, G. Amjad, and L. Younesi, "Application of Imaging Technologies in Breast Cancer Detection: A Review Article," *Open Access Maced. J. Med. Sci.*, vol. 7, no. 5, p. 838, Mar. 2019, https://doi.org/10.3889/oamjms.2019.171.

BIOGRAPHY OF AUTHORS

Herry Tony Andhyka was born in Jakarta, Indonesia, on 12 November 1999. He entered Universitas Indonesia in 2017 and graduated in 2021 with a Bachelor of Engineering Degree. He currently takes Magister Program at Universitas Indonesia, majoring in Telecommunication Engineering in the third semester. His main research interest includes an antenna and terahertz propagation.

Catur Apriono (Member, IEEE) received the B.Eng. and M.Eng. degrees in telecommunication engineering from the Department of Electrical Engineering, Universitas Indonesia, Indonesia, in 2009 and 2011, respectively, and the Ph.D. degree in nano vision technology from Shizuoka University, Japan, in 2015. Since 2018, he has been an Assistant Professor of telecommunication engineering with the Universitas Indonesia, where he is currently a Lecturer with the Department of Electrical Engineering, Faculty of Engineering. His main research interests include antenna and microwave engineering, terahertz wave technology, and optical communications. He has been a member of the IEEE Antenna and Propagation Society (AP-S) and the IEEE Microwave Theory and Technique Society (MTT-S). He has had involvement in the IEEE Joint Chapter MTT/AP Indonesia Section as a Secretary and a Treasurer in 2017, 2018, and 2019, and various chapter activities, such as the First Indonesia–Japan Workshop on Antennas and Wireless Technology (IJAWT) as a Secretary and the 2019 IEEE International Conference on Antenna Measurements Applications (CAMA), Bali, in October 2019, as a Treasurer.

Fitri Yuli Zulkifli (SM IEEE) received her degree in electrical engineering for Bachelor (1997) and PhD (2009) from Universitas Indonesia (UI), while MSc degree from Karlsruhe Institute of Technology, Germany (2002). Her research interests are Antenna, Propagation, Microwave and in the field of Telecommunication. She joined the Antenna Propagation and Microwave Research Group (AMRG) UI since 1997 and has become lecturer in electrical engineering department UI since 1998. Prof. Yuli has published more than 200 papers in journals/conference proceedings and received more than 40 research grants. She now leads "Laboratory Prof. Fitri Yuli Zulkifli" and also the head of professional engineering study program in UI. From 2011-2012 she became the joint chapter chair of MTT/AP Indonesia. In 2017-2018, she was the IEEE Indonesia Section Chair and in 2019-2022, she serves as committee member for R10 Conference and Technical Seminar and Conference Quality Management.